Available online at www.sciencedirect.com
ScienceDirect
Journal of Hazardous Materials 152 (2008) 48–55
Journal of Hazardous Materials
www.elsevier.com/locate/jhazmat

A visible light response TiO_2 photocatalyst realized by cationic S-doping and its application for phenol degradation

Shouxin Liu *, Xiaoyun Chen [1]

College of Material Science and Engineering, Northeast Forestry University, Harbin 150040, Heilongjiang, China

Received 11 February 2007; received in revised form 17 June 2007; accepted 18 June 2007
Available online 22 June 2007

Abstract

S-doped TiO_2 photocatalyst with high visible light activity was prepared by acid catalyzed hydrolysis method using thiourea (TU) as sulfur source. The catalyst was characterized by DRS, XPS, XRD, FTIR, SEM and N_2 adsorption. It was found that cation S^{6+} was homogeneously incorporated into the bulk phase of TiO_2 and substitutes for some of the lattice titanium (Ti^{4+}). Doped S can form a new band above the valence band and narrow the band-gap of the photocatalyst, giving rise to a second absorption edge in the visible light region. The activity of the catalyst was examined by photodegradation of phenol in aqueous solution under both artificial visible light and solar light irradiation. The activity of catalyst was found to be dependent on the doping amount of S and the maximum activity was observed when the catalyst was obtained by calcinated at 600 °C with the mass ratio of $TU/TiO_2 = 1$. Too much of new-generated band-gap structures due to higher S-doping could act as recombination centers for electron–hole pairs. Catalyst with optimum S-doping exhibited the highest activity under both artificial light and solar irradiation for phenol degradation. In addition, doped S also beneficial for the better dispersion, large S_{BET} and phase transformation retardation of TiO_2.

Keywords: Sulfur cation-doped TiO_2; Visible light; Phenol degradation; Mechanism

1. Introduction

Heterogeneous photocatalysis by TiO_2 semiconductors is promising for elimination of hazard environmental pollutants [1–5], especially for the degradation of biorecalcitrant organic contaminants. However, the TiO_2 photocatalyst has not been applied widely in the field of environmental pollution control, since its large band-gap energy ($E_g = 3.2$ eV) considerably limits the utilization of natural solar light or artificial visible light. Traditional visible light responsive catalysts are unstable under illumination (such as CdS and CdSe) or have low activity (such as WO_3 and Fe_2O_3) [6]. Modification of TiO_2 to extend its absorption edge toward the visible light region has been the subject of recent research. Some UV-active oxides were used as visible-light photocatalysts by substitution doping of metal ions [7,8], ion implantation [9], organic dye sensitization [10], hydrogen plasma reduction of TiO_2 [11], and hydroxide or surface coordination [12]. However, these modified photocatalysts, in general, show a weak absorption in the visible light region and deactivate easily [13]. Band-gap narrowing by the introduction of nonmetal anions (N, C, S and F) into TiO_2 was recently found to be more efficient than the traditional methods to yield catalyst with high catalytic activity under visible light irradiation [13–22].

Several works concerning nonmetal cations doping was reported. Ohno reported that S cation-doped TiO_2 powder absorbed visible light more strongly than N, C and the S anion-doped TiO_2 powders and showed photocatalytic activity under visible light [13]. They demonstrated that the substitution of Ti^{4+} by S^{4+} was responsible to the visible light absorbance. Previous study reported that if TU was used, the substitution of Ti^{4+} by S^{6+} would be more favorable than replacing O^{2-} with S^{2-} [13,23,24]. In addition, Ihara et al. [25] indicated that the grain boundary (13 nm) is important for the visible light activity of the TiO_2 photocatalyst. The acid-catalyzed hydrolysis method is effective for the preparation of TiO_2 particles with a size of 10–13 nm [16,26].

In this work, with the aim of developing a high efficient photocatalyst which can be used in hazardous treatment

* Corresponding author. Tel.: +86 451 82191204; fax: +86 451 82191204.
E-mail addresses: liushouxin@126.com (S. Liu), chenxy_dicp@126.com (X. Chen).
[1] Tel.: +86 451 82191204; fax: +86 451 82117883.

0304-3894/$ – see front matter © 2007 Elsevier B.V. All rights reserved.
doi:10.1016/j.jhazmat.2007.06.062

field, the acid-catalyzed hydrolysis method was adopt and TU was used as raw material for the preparation of visible light response S cation-doped TiO_2 photocatalysts with controlled size (10–13 nm). The catalyst was characterized by DRS, XPS, XRD, FTIR, SEM and N_2 adsorption and the activity was examined by photodegradation of phenol in aqueous solution under both artificial and natural visible light irradiation. Based on the result of photocatalyst characterization and activity test, the catalytic mechanism was also discussed.

2. Experimental

2.1. Preparation of the S-doped TiO_2 photocatalyst

In an ice bath [16], 25 ml $TiCl_4$ was added dropwise into 250 ml H_2O under vigorous stirring at 5 °C for 1 h. A solution mixture of $(NH_4)_2SO_4$ and HCl was then added and further stirred for 0.5 h, and the $TiCl_4$:$(NH_4)_2SO_4$:HCl molar ratio was maintained at 1:2:10 during the reaction. The mixture was heated to 98 °C at a rate of 5 °C/min and was maintained at this temperature for 1 h. Thereafter, $NH_3{\cdot}H_2O$ was used to adjust the pH to 8 and the mixture was kept at 98 °C for 1 h. The TiO_2 precursor thus obtained was aged at room temperature for 10 h and then washed with double-deionized water until no Cl^- was detected, followed by washing with ethanol. Finally, the prepared TiO_2 precursor was added into the mixture of TU and ethanol (with mass ratio of TiO_2 to TU: 1:0.25, 1:0.5, 1:1, 1:1.5, 1:2, 1:3), stirred for 1 h and aged for 12 h, then vacuum dried at 85 °C for 6 h. The obtained powder was grounded and placed in a quartz reactor, then heated under air atmosphere with a ramp rate of 20 °C/min to a certain temperature (500, 600, 700 and 800 °C, respectively) and maintained for 2 h. For comparison, the unmodified TiO_2 was prepared under otherwise the identical conditions in the absence of TU.

2.2. Characterization of photocatalyst

The surface composition and valence state of the obtained photocatalysts were detected by a PHI5700 X-ray photoelectron spectroscopy using Al Kσ X-ray ($h\nu = 1486.6$ eV). The binding energy was referenced to the C_{1s} line at 284.6 eV for calibration. Ti/O atomic ratio of the S-doped TiO_2 was determined by the peak intensities of Ti_{2p} and O_{1s}. The surface structure of the photocatalyst was observed using a QUANTA 200 scanning electron microscope. XRD analysis was performed on a D/max-rB X-ray diffractometer with Cu Kα radiation (45 kV, 40 mA). The TiO_2 crystallite size was calculated from the Scherrer equation, and the content of anatase was determined according to the following equation:

$$w_A = \frac{1}{1 + I_R/(KI_A)}$$

where w_A is the content of the anatase, I_R and I_A are the intensities of the diffraction peaks of rutile and anatase, respectively, and K is the Scherrer constant. FTIR analysis was conducted on a Nicolet MAGNA 560 spectrophotometer using a KBr pellet for sample preparation. The specific surface area of the sample was measured using an ST-2000 automated apparatus based on the Brunauer–Emmett–Teller (BET) method at −196 °C with N_2 as the adsorbent and H_2 as the carrier gas.

2.3. Photocatalytic activity test

The artificial light photocatalytic activity test was carried out in a cylindrical quartz photoreactor (275 ml) using phenol as the model compound. A 380-W Xe lamp ($\lambda_{max} = 510$ nm, $\lambda < 410$ nm was cut off by a UV filter) positioned inside the reactor as the irradiation source. Photocatalyst powder (0.25 g) was added to 250 ml aqueous solution of phenol (100 mg/l). Before the photocatalytic degradation, the suspension was magnetically stirred in the dark for 30 min to establish a phenol adsorption/desorption equilibrium. Samples of 5 ml were collected from the suspension and were immediately centrifuged at 4000 r/min for 10 min. The concentration of phenol after illumination was determined spectrophotometrically at 270 nm using a TU-1900 UV spectrometer.

Experiments using solar irradiation were carried out from 9:10 a.m. to 5:30 p.m. during the autumn season in Harbin and Petri dishes with 15 cm diameter were used as reactor. Each Petri dish contained a 100 ml of 50 mg/l phenol aqueous solution and 0.1 g photocatalyst. The Petri dishes were covered with plastic film to prevent evaporation of phenol solution. As artificial light activity test, before the photocatalytic degradation, the suspension was magnetically stirred in the dark for 30 min to establish a phenol adsorption/desorption equilibrium. Then the covered Petri dishes were placed under direct sunlight. During the irradiation experiments, neither forced aeration nor stirring of phenol solution was conducted.

3. Results and discussion

3.1. Result of XPS

The XPS spectra of S-doped TiO_2 and naked TiO_2 and their deconvolution with a Gaussian function are presented in Fig. 1. Eight peaks of $Ti_{2p_{1/2}}$, $Ti_{2p_{3/2}}$, Ti_{2s}, Ti_{3s}, Ti_{3p}, O_{1s}, S_{2p} and C_{1s} were appeared for S-doped TiO_2. C_{1s} peak at 284.6 eV were organic polluted carbon and used for calibration. S_{2p} and Ti_{2p} spectra was shown as Fig.1(b) and (c), respectively. The oxidation state of the S-dopant is dependent on the preparation routes and sulfur precursors. Previous study reported that if TU was used, the substitution of Ti^{4+} by S^{6+} would be more favorable than replacing O^{2-} with S^{2-} [13,23,24]. S_{2p} spectra can be resolved into four peaks, ${S_{2p_{1/2}}}^{6+}$, ${S_{2p_{3/2}}}^{6+}$, ${S_{2p_{1/2}}}^{4+}$ and ${S_{2p_{3/2}}}^{4+}$. It is clear that S was doped mainly as S^{6+}, the content of S^{4+} was much lower and no S^{2-} was detected. When the S-doped samples were washed with water repeatedly, the intensity and binding energy of S^{6+} remained. This revealed that doped S was not formed in the form of sulfur oxides on TiO_2 surface. From Fig. 1(c), the binding energies of $Ti_{2p_{1/2}}$ and $Ti_{2p_{3/2}}$ were observed to be at 464.5 and 458.7 eV, which should be assigned to Ti^{4+} of TiO_2. It is obvious that the doped S can lead to the peak of $Ti_{2p_{1/2}}$ and $Ti_{2p_{3/2}}$ shift to the lower binding energy. This may

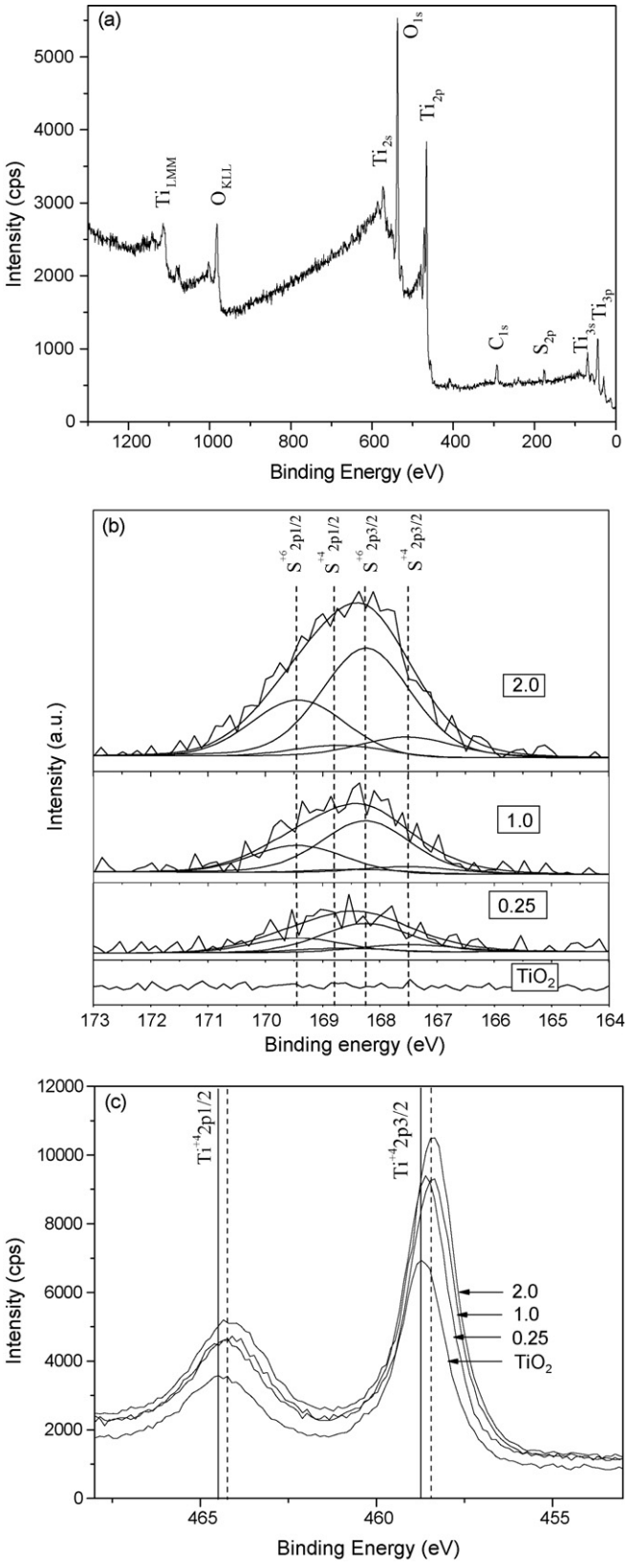

Fig. 1. XPS spectra (a), S_{2p} spectra (b) and Ti_{2p} spectra (c) of S-doped TiO_2 (calcinated at 600 °C) with different TU/TiO_2 ratios.

Table 1
XPS elements analysis result of $Ti_{1-x}S_yO_2$ calcinated at 600 °C with different mass ratio of TU to TiO_2

Sample TU/TiO_2	w (Ti) (%)	w (O) (%)	w (S) (%)	m(Ti):m(O)
TiO_2	28.39	71.61	0.00	39.65:100
0.25	28.01	71.54	0.45	39.15:100
1.0	27.38	71.63	0.99	38.22:100
2.0	25.98	71.56	2.42	36.31:100

be caused due to the difference of ionization energy of Ti and S. The Ti:O atomic ratio based on XPS spectrum decreased when S-doping increased (Table 1). Therefore, it could be concluded that the lattice titanium sites of TiO_2 were substituted by S^{6+} and formed a new band energy structure.

3.2. Result of DRS

Diffuse reflectance spectra of S-doped TiO_2 with different mass ratio of TU/TiO_2 (a) and its first derivative (b) are shown in Fig. 2. Like reported anion nonmetal doped TiO_2 [13–22], a second absorption edge in the visible region (490–550 nm) appeared for all prepared S-doped TiO_2, indicating that more photons can effectively be utilized by catalyst excitation. It is thought that the first and second edges are related to the band-gap of the original TiO_2 and the S-doped sample, respectively. With the increase of S-doping content, the second absorbance edge shifts to the longer wavelength and the visible light absorbance increased.

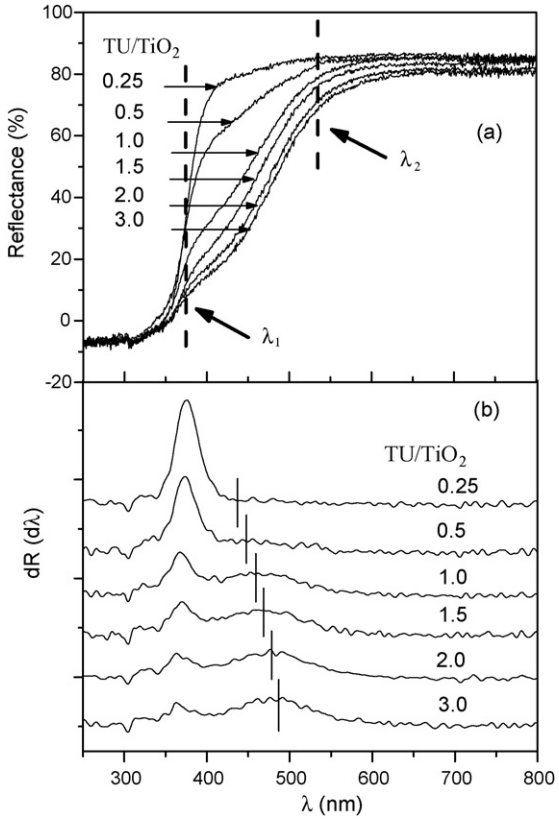

Fig. 2. (a) Diffuse reflectance spectra of S-doped TiO_2 catalysts with different mass ratio of TU to TiO_2 (calcinated at 600 °C). (b) The first derivative of (a).

Table 2
Characteristics of TiO_2 and S-doped TiO_2 catalyst

Sample TU/TiO_2 (calcination temperature (°C))	Crystalline size (nm)	S_{BET} ($m^2\ g^{-1}$)	1st adsorption edge λ_{1max} (nm)	1st $E_{band\text{-}gap}$ (eV)	2nd adsorption edge λ_{2max} (nm)	2nd $E_{band\text{-}gap}$ (eV)
TiO_2	13.0	58.37	380	3.2	–	–
0.25 (600 °C)	–	55.41	375.03	3.306	453.83	2.732
0.5 (600 °C)	–	46.83	375.85	3.299	458.77	2.703
1.0 (600 °C)	14.0	40.47	374.35	3.312	466.71	2.657
1.5 (600 °C)	–	38.55	376.04	3.298	473.61	2.618
2.0 (600 °C)	–	35.82	375.13	3.306	482.67	2.569
3.0 (600 °C)	–	30.47	377.11	3.288	490.46	2.528
1.0 (400 °C)	9.0	71.48	376.39	3.294	466.91	2.665
1.0 (500 °C)	12.0	69.15	374.63	3.310	466.52	2.658
1.0 (700 °C)	21.0	26.41	373.94	3.316	448.97	2.762
1.0 (800 °C)	32.0	15.57	375.66	3.301	–	–

The appearance of the second absorption edge showed that a new energy band was formed. This may suggest that the substitution of lattice titanium by cation S^{6+} can formed an isolated narrow band above the valence band of TiO_2 and narrowed the band-gap, then produce a second absorption edge in the visible region (490–550 nm). The 1st and 2nd band-gap energy of all S-doped catalysts were calculated according to the equation of $E_g = 1240/\lambda$ [16], the results were listed as Table 2.

DRS result of S-doped TiO_2 samples calcinated at different temperatures ($TU/TiO_2 = 1$) were present in Fig. 3. When calcinated lower than 600 °C, all samples exhibited almost similar absorption edge and visible light absorbance. The second absorption edge shifted to shorter wavelength when the sample calcinated at 700 °C. With the increasing of calcination temperature, the yellowish color of the obtained catalysts gradually disappeared. When calcinated at 800 °C, the obtained S-doped TiO_2 exhibited the same color and absorption edge with naked TiO_2 and no visible photo-response could be observed.

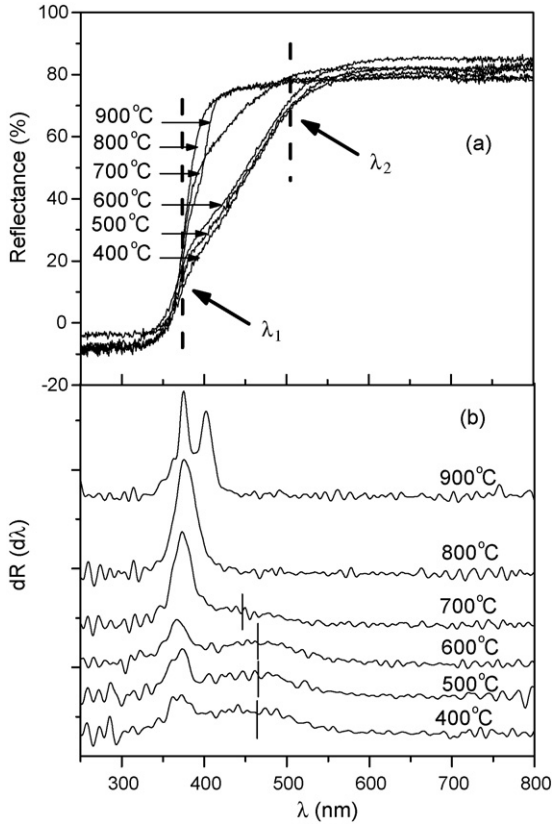

Fig. 3. Diffuse reflectance spectra of S-doped TiO_2 calcinated at different temperatures ($TU/TiO_2 = 1$). (b) The first derivative of (a).

3.3. Result of XRD

The XRD patterns of S-doped TiO_2 calcinated at different temperatures (Fig. 4) showed that no significant shift of the characteristic peaks of anatase or rutile was observed, this may be caused due to the amount of S-doping is trivial. However, S-doping can inhibited phase transformation of TiO_2 from anatase to rutile. For S-doped TiO_2, the amorphous precursor was almost completely transformed into anatase at 400 °C and exhibited a well-crystallized anatase with a distinct peak at $2\theta = 25.2°$ when calcinated at 500 °C. The phase transformation of anatase to rutile started at 800 °C, which is much lower than naked TiO_2. When calcinated at 900 °C, 37 wt% anatase was observed for the S-doped TiO_2. For the naked TiO_2, however, the phase transformation of anatase to rutile started at 700 °C and almost completely (97 wt% rutile) transformed to rutile at 800 °C.

The physical parameters of S-doped TiO_2 and naked TiO_2 are summarized in Table 2. Fig. 5 shows the influence of calcination temperatures on the surface area and crystallite size of the catalyst. With the increasing of the calcination temperature, the surface area decreased and the crystallite size increased. In comparison with the naked TiO_2, the rate of crystallite growth and S_{BET} decrease of S-doped samples was slower. It is obvious that doped S is contributed to the small particle size and the large surface area of the catalyst.

3.4. Result of FTIR

Result of FTIR analysis was shown Fig. 6. It is obvious that four main absorption peaks located at 3480, 1600, 1030

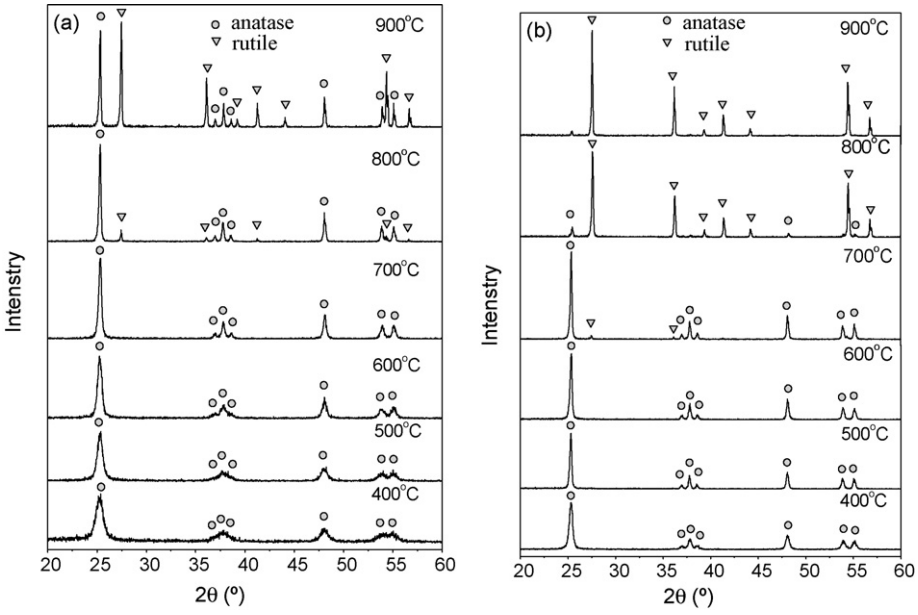

Fig. 4. XRD pattern of S-doped (TU/TiO_2 = 1) TiO_2 (a) and TiO_2 (b) calcinated at different temperatures.

and 530 cm^{-1} appeared for S-doped samples. The peaks at 3480 and 1600 cm^{-1} should assigned to the stretching vibration and bending vibration of surface –OH group and 530 cm^{-1} to Ti–O stretching vibration. Compared with naked TiO_2, S-doping seems has no effect on the quantity and properties of surface –OH. The shift to the lower wavenumbers and sharpening of Ti–O peaks may due to the size decrease and phase transformation. The appearance of the peak at 1031 cm^{-1} is an indicative of a new interaction of Ti–O–S. The characteristic peak of the Ti–O–C bond on the interface of TiO_2 and the activated carbon appeared at 1020 cm^{-1} [26], Ti–O–N bond of N-doped TiO_2 emerged at 1060 cm^{-1} [16] and that of the Ti–O–Si bond on the TiO_2/SiO_2 composite catalyst at 949 cm^{-1} [27]. Considering the electron affinity of S, C, N and Si, the peak at 1030 cm^{-1} should be related to Ti–O–S, suggesting a conjugation effect between the S and Ti–O bonds.

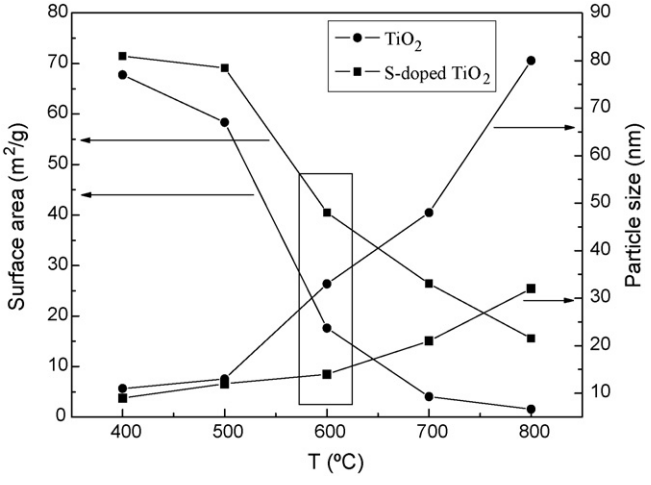

Fig. 5. Effect of calcination temperature on the S_{BET} and crystalline size of S-doped (TU/TiO_2 = 1) TiO_2 and TiO_2.

3.5. Result of SEM

SEM images of calcinated S-doped TiO_2 at different temperatures were presented in Fig. 7. Combined with the result of XRD, it is obvious that the agglomeration was significant for unmodified TiO_2, the agglomerate size was 400–500 nm for the 500 °C calcinated catalyst. However, S-doping can improve the dispersion and reduce the agglomerate size of TiO_2. The agglomerate size was 50–100 nm for the 700 °C calcinated S-doped TiO_2.

3.6. Photocatalytic activity

Figs. 8 and 9 showed the relative concentration of phenol, C/C_0, for different times during the artificial visible light irradiation of S-doped TiO_2 photocatalyst prepared by different mass ratio of TU/TiO_2 and calcination temperatures. It is clear that S-doping can increase the visible light activity. The visible light

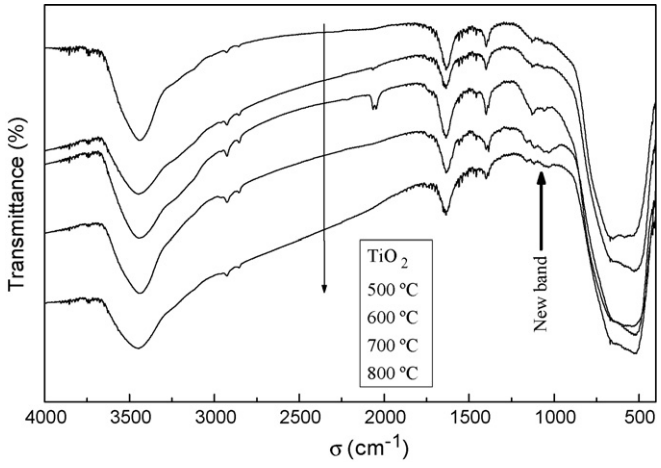

Fig. 6. FTIR spectra of TiO_2 and S-doped TiO_2 catalysts (TU/TiO_2 = 1).

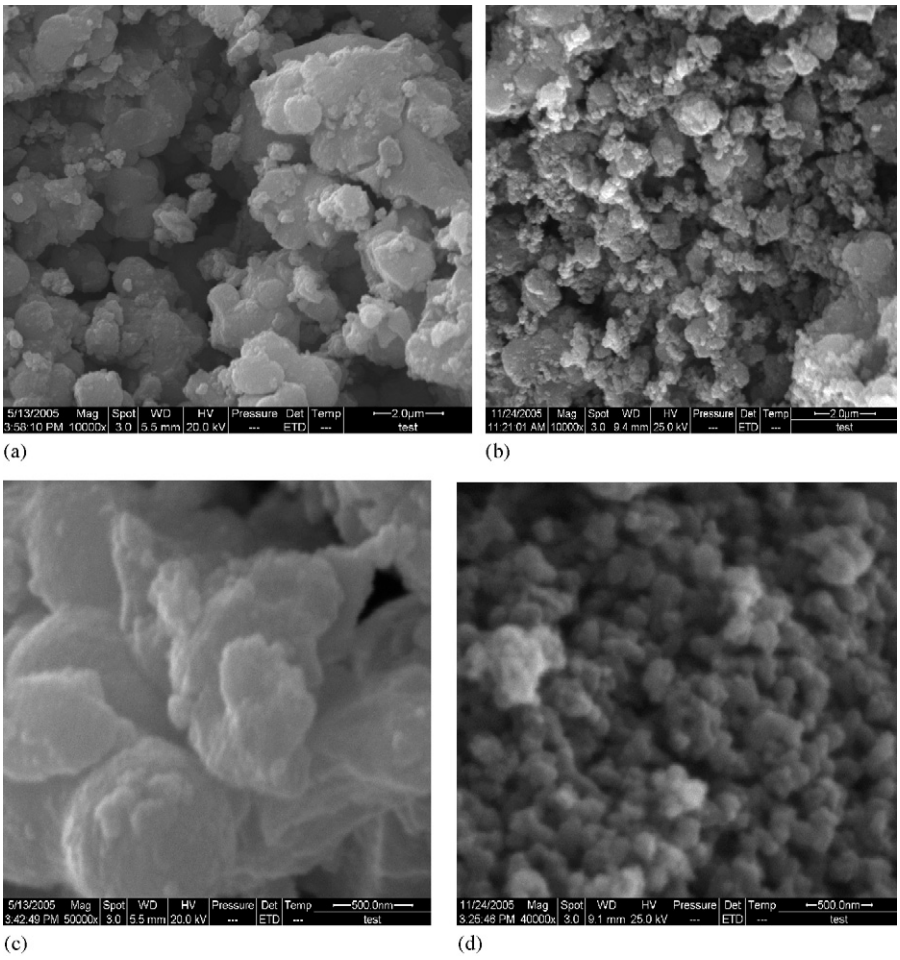

Fig. 7. SEM images of TiO_2 and S-doped TiO_2 prepared at different calcination temperatures ($TU/TiO_2 = 1$). (a) TiO_2, 500 °C. (b) S-doped TiO_2, 500 °C. (c) TiO_2, 700 °C. (d) S-doped TiO_2, 700 °C.

activity was not proportional to the S-doping and visible absorption, however, an optimum amount of doping S existed. With the increasing of S-doping, the activity increased up to the mass ratio of $TU/TiO_2 = 1$ then decreased. The result of Fig. 8 indicated that 600 °C is the optimum calcinations temperature. S-doped TiO_2 ($TU/TiO_2 = 1$ and calcinated at 600 °C) showed the maximum activity among all the samples, which can effectively degrade phenol within 60 min. On the other hand, only 21%

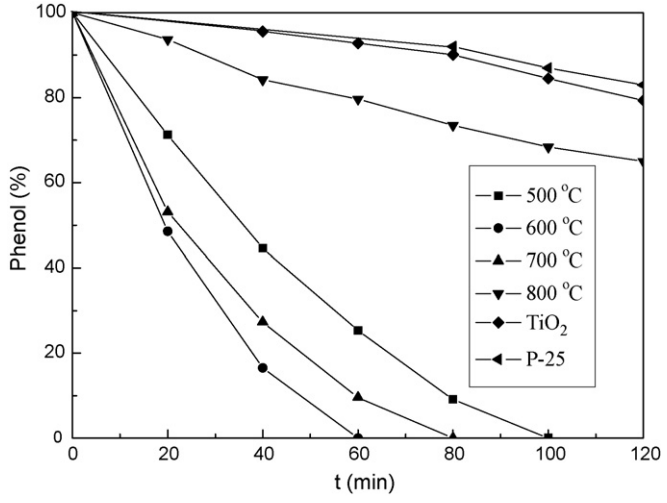

Fig. 8. Photocatalytic activity of TiO_2 and S-doped TiO_2 calcinated at different temperatures ($TU/TiO_2 = 1$).

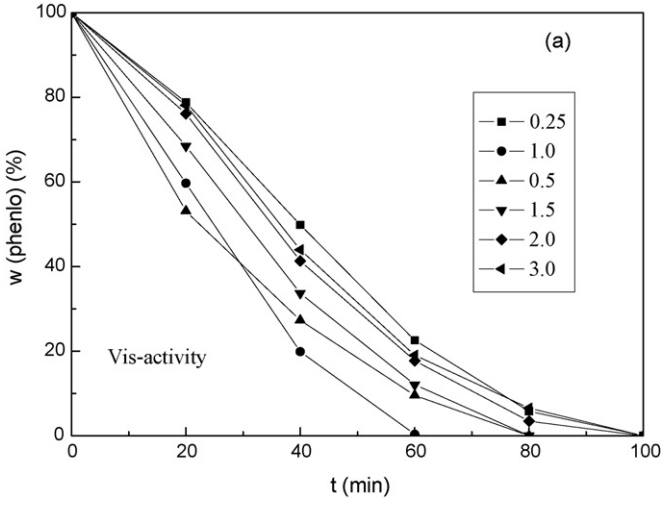

Fig. 9. Photocatalytic activity of S-doped TiO_2 with different mass ratio of TU to TiO_2 (calcinated at 600 °C).

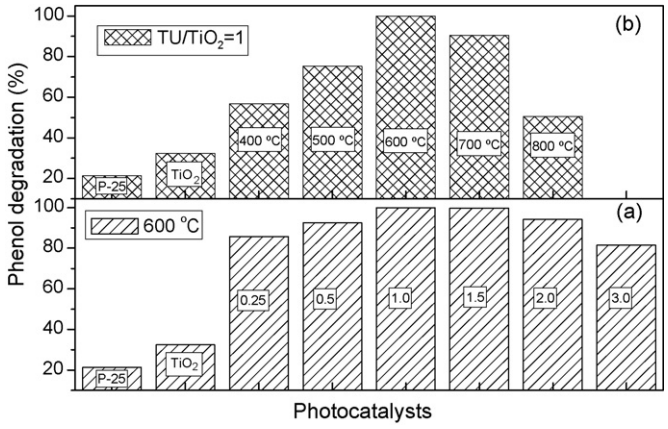

Fig. 10. Photocatalytic activity of TiO_2 and S-doped TiO_2 under solar light: (a) S-doped TiO_2 with different TiO_2 to TU mass ratio (calcinated at 600 °C); (b) S-doped TiO_2 calcinated at different temperatures ($TU/TiO_2 = 1$).

and 17% phenol were degraded on naked TiO_2 and commercial P-25, respectively, under otherwise the identical condition. It can be seen from Fig. 10, when solar irradiation was adopted, the optimum ratio of $TU/TiO_2 = 1$ and 1.5 and the calcination temperature was 600 °C. The S-doped TiO_2 photocatalyst prepared under the optimum condition can reach almost 100% phenol removal under solar irradiation. However, for naked TiO_2 and commercial P-25, the phenol degradation was less than 35% and 21%, respectively. Combined above activity and DRS result, it can be seen that the visible light activity was not directly proportional to the red shift of the second absorption edge and visible light absorbance.

For the S-doped TiO_2 powders obtained in this work, the visible-light photocatalytic activity was independent of the visible-light absorbance and an optimum S-doped content existed. While the visible light absorbance correlated with doped S content. XPS and DRS result showed that the substitution of lattice titanium by S atoms can form an isolated narrow band above the valence band and narrow the band-gap, and then produce a second absorption edge in the visible region. However, with the increasing of the S-doped content, the position of the new-generated band-gap structures elevated and then could act as recombination centers for electron–hole pairs [16,25]. The mechanism of dope-S for the visible-light activity was illustrated as Fig. 11.

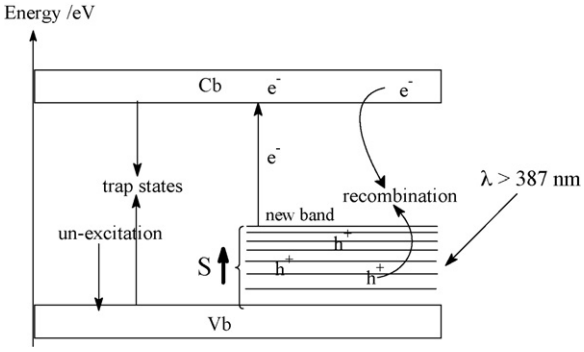

Fig. 11. Mechanism of S-doped TiO_2 for the visible-light activity photocatalyst.

4. Conclusion

S-doped TiO_2 photocatalyst with high activity for phenol degradation under visible light illumination can be obtained by acid catalyzed hydrolysis method using TU as sulfur source. Cationic S^{6+} is incorporated into the bulk phase of TiO_2 and substitutes for partial titanium (Ti^{4+}). The visible-light photocatalytic activity of S-doped TiO_2 was independent of the absorption edge. While the visible light absorbance correlated with doped S content. Doped S can form a new band-gap, giving rise to a second adsorption edge at 450–550 nm which can be excited by visible light. However, too much new-generated band-gap structures could act as recombination centers for electron–hole pairs. In addition, doped S also beneficial for TiO_2 crystalline dispersion, large S_{BET} and phase transformation retardation.

Acknowledgements

This project was financially supported by the Program for New Century Excellent Talents in University, the Specialized Research Fund for the Doctoral Program of Higher Education (No. 20050225006) and the National Natural Science Foundation of China (No. 30400339).

References

[1] J. Matos, J. Laine, J.M. Herrman, Synergy effect in the photocatalytic degradation of phenol on a suspended mixture of titania and AC, Appl. Catal. B: Environ. 18 (1998) 281–285.
[2] J.M. Herrman, J. Matos, J. Disdier, et al., Solar photocatalytic degradation of 4-chlorophenol using the synergistic effect between titania and AC in aqueous suspention, J. Catal. Today 3 (1999) 54–60.
[3] M.R. Hoffmann, S.T. Martin, W.Y. Choi, et al., Environmental applications of semiconductor photocatalysis. Chemical reviews, Chem. Rev. 95 (1995) 69–76.
[4] A.L. Linsebiger, G.Q. Lu, J.T. Yates, Photocatalysis on TiO_2 surfaces: principles, mechanisms, and selected results, Chem. Rev. 95 (1995) 735–758.
[5] S.X. Liu, Z.P. Qu, X.W. Han, et al., A mechanism for the enhanced photocatalytic activity of silver loaded titanium dioxide, Catal. Today 93 (2004) 877–884.
[6] K. Kobayakawa, Y. Murakami, Y. Sato, Visible-light active N-doped TiO_2 prepared by heating of titanium hydroxide and urea, J. Photochem. Photobiol. A: Chem. 170 (2005) 177–246.
[7] S.X. Liu, Z.P. Qu, X.W. Han, et al., Effect of silver modification on the photocatalytic activity of TiO_2 photocatalysis, Chin. J. Catal. 25 (2004) 133–138.
[8] H. Haick, Y. Paz, Long-range effects of noble metals on the photocatalytic properties of titanium dioxide, J. Phys. Chem. B 107 (2003) 2319–2326.
[9] M. Anpo, M. Takeuchi, The design and development of highly reactive titanium oxide photocatalysts operating under visible light irradiation, J. Catal. 216 (2003) 505–516.
[10] B.O. Regan, M. Gratzel, A low-cost, high-efficiency solar cell based on dye-sensitized colloidal TiO_2 films, Nature 353 (1991) 737–740.
[11] I. Nakamura, N. Negishi, S. Kutsuna, et al., Role of oxygen vacancy in the plasma-treated TiO_2 photocatalyst with visible light activity for NO removal, J. Mol. Catal. A: Chem. 161 (2000) 205–212.
[12] T. Ihara, M. Miyoshi, Y. Iriyama, et al., Visible-light-active titanium oxide photocatalyst realized by an oxygen-deficient structure and by nitrogen doping, Appl. Catal. B: Environ. 42 (2003) 403–409.
[13] T. Ohno, M. Akiyoshi, T. Umebayashi, et al., Preparation of S-doped TiO_2 photocatalysts and their photocatalytic activities, Appl. Catal. A: Gen. 265 (2004) 115–123.

[14] T. Umebayashi, T. Yamaki, H. Itoh, et al., Band gap narrowing of titanium dioxide by sulfur doping, Appl. Phys. Lett. 81 (2002) 454–456.
[15] R. Gómez, T. López, E. Ortiz-Islas, et al., Effect of sulfation on the photoactivity of TiO_2 sol–gel derived catalysts, J. Mol. Catal. A: Chem. 193 (2003) 217–226.
[16] S.X. Liu, X.Y. Chen, X. Chen, N-doped visible light response nanosize TiO_2 photocatalyst prepared by acid catalyzed hydrolysis method, Chin. J. Catal. 27 (2006) 697–702.
[17] H. Irie, Y. Watanabe, K. Hashimoto, Nitrogen-concentration dependence on photocatalytic activity of TiO_2–xN_x powders, J. Phys. Chem. B 107 (2003) 5483–5486.
[18] H. Irie, Y. Watanabe, K. Hashimoto, Carbon-doped anatase TiO_2 powders as a visible-light sensitive photocatalyst, Chem. Lett. 32 (2003) 772–773.
[19] S.U.M. Khan, M. Al-Shahry, W.B. Ingler Jr., Efficient photochemical water splitting by a chemically modified n-TiO_2, Science 297 (2002) 2243–2245.
[20] T. Umebayashi, T. Yamaki, S. Tanaka, K. Asai, Visible light-induced degradation of methylene blue on S-doped TiO_2, Chem. Lett. 32 (2003) 330–332.
[21] T. Umebayashi, T. Yamaki, H. Itoh, K. Asai, Band gap narrowing of titanium dioxide by sulfur doping, Appl. Phys. Lett. 81 (2002) 454–456.
[22] I. Justicia, P. Ordejon, G. Canto, Designed self-doped titanium oxide thin films for efficient visible-light photocatalysis, Adv. Mater. 14 (2002) 1399–1402.
[23] T. Ohno, T. Mitsui, M. Matsumura, Photocatalytic activity of S-doped TiO_2 photocatalyst under visible light, Chem. Lett. 32 (2003) 364–366.
[24] T. Ohno, Preparation of visible light active S-doped TiO_2 photocatalysts and their photocatalytic activities, Water Sci. Technol. 49 (2004) 159–163.
[25] R. Asahi, T. Morikawa, T. Ohwaki, et al., Visible-light photocatalysis in nitrogen-doped titanium oxides, Science 293 (2001) 269–271.
[26] X.Y. Chen, S.X. Liu, X. Chen, et al., Characterization and activity of TiO_2/xAC composite photocatalyst prepared by acid catalyzed hydrolysis method, Acta Phys. Chim. Sin. 22 (2006) 517–521.
[27] X. Zhang, F. Zhang, K.Y. Chan, Visible-light sensitization of TiO_2 photocatalysts by wet-method N doping, Appl. Catal. A: Gen. 284 (2005) 193–202.